PHYSICAL REVIEW B **79**, 054201 (2009)

Augmented-space cluster coherent potential approximation for binary random and short-range ordered alloys

Moshiour Rahaman
Department of Materials Science, S.N. Bose National Centre for Basic Sciences, JD Block, Sector III,
Salt Lake City, Kolkata 700098, India

Abhijit Mookerjee*
Advanced Materials Research Unit, S.N. Bose National Centre for Basic Sciences, JD Block, Sector III,
Salt Lake City, Kolkata 700098, India

(Received 4 December 2008; published 5 February 2009)

We use the earlier ideas of Razee and Prasad [Phys. Rev. B **45**, 3265 (1992); Phys. Rev. B **48**, 1349 (1993)], Datta *et al.* [Phys. Rev. B **48**, 8567 (1993)], and Mookerjee and Prasad [Phys. Rev. B **48**, 17724 (1993)] to propose and implement a cluster generalization of the coherent potential approximation within a tight-binding linear muffin-tin orbital minimal basis set for binary alloys which are either random or have short-range order. In particular, we shall apply the technique to the CuZn alloys and compare it with other approaches.

DOI: 10.1103/PhysRevB.79.054201 PACS number(s): 36.40.Cg, 75.50.Pp

I. INTRODUCTION

The search for successful approximations for the study of configuration averaging in disordered systems and ones which preserve the Herglotz analytic properties[1] and lattice translational symmetry of the averaged Green's functions has thrown up several alternative approaches. These methods of dealing with disorder fall into four categories:

(1) To the first category belongs the single-site mean-field coherent potential approximation (CPA). This approximation has been eminently successful in dealing with a variety of disordered systems.

(2) To the second category belong the generalizations of the CPA, of which the augmented-space-based methods—the cluster coherent potential approximation (CCPA) suggested by Razee and Prasad,[2,3] the itinerant coherent potential approximation (ICPA) of Ghosh *et al.*,[4] and the augmented-space recursion (ASR) (Ref. 5)—are foremost. They not only retain the necessary analytic (Herglotz) properties and lattice translational symmetry of the averaged Green's function, as the CPA does, but also properly incorporate local environment effects.

(3) To the third category belong the supercell-based calculations. Zunger *et al.*[6] suggested that if we construct a supercell and populate its lattice points randomly by the constituents so as to mimic the concentration correlations in the random alloy, a single calculation with this superlattice should approximate the configuration average in the infinite random system.

The above methods are essentially real-space approaches. There is a fourth class of techniques based on reciprocal-space renormalization: the nonlocal coherent potential approximation (NL-CPA). The underlying idea was first suggested by Jarrell and Krishnamurthy[7] and applied to CuZn alloys by Rowlands *et al.*[8] The method is capable of taking into account environmental effects and short-range ordering.

Of all the single-site approximations, the CPA alone maintains the essential Herglotz analytical properties and lattice translational symmetry of the averaged Green's function. However, either whenever there is strong scattering due to disorder-induced configuration fluctuations, as in dilute split-band alloys, or when local environment effects such as short-range ordering, clustering and segregation, or local lattice distortions due to size mismatch of the constituent atoms become important, the single-site-based CPA becomes inadequate.

The aim of this paper is to extend the ideas suggested by Razee and Prasad[2,3] to realistic alloys and apply it to CuZn as a test case. The basic idea behind our method is to look at a particular site in the lattice (it does not matter which), and then estimate the effect of its random environment on a local electronic property at that site. Homogeneity of disorder ensures that the environment of any site is statistically equivalent to that of all others. We retain the randomness of the immediate environment and replace the far environment by an effective medium. The effect of the environment is obtained by downfolding it onto the chosen site using the partitioning theorem.[9] The ASR has a very similar approach: choosing a site to begin recursion and then repeatedly downfolding further and further environments[10,11] onto it. The main difference between the two approaches is the way in which the far environment is estimated. In the ASR we do it through the "terminating" procedure,[12] while in the CCPA we approximate it with an effective medium which is self-consistently generated using mean-field ideas.[13] We should note that our approach is different from the embedded-cluster approaches,[14,15] where the cluster is embedded in a CPA medium with no attempt to generate it self-consistently.

The paper will be arranged as follows: in Sec. II we shall introduce the tight-binding linear muffin-tin orbital (TB-LMTO) for substitutionally disordered binary alloys. In Sec. III we shall briefly describe the augmented-space formalism on which the subsequent CCPA will depend. In Sec. IV we shall explicitly describe the CCPA in great detail for homogeneous perfectly random disorder. In Secs. V and VI we shall modify our methodology to incorporate short-range order (SRO) and off-diagonal disorder, respectively. Finally in Sec. VII we shall apply the developed methodology to equiatomic CuZn alloys and compare our results with other approaches.

II. TB-LMTO-ASR FORMALISM FOR BINARY ALLOYS

Our study of the electronic structure of disordered binary alloys will begin with the solution of the Kohn-Sham equation,[16] where the effective one-electron Hamiltonian will be represented in the minimal basis set of a tight-binding linear muffin-tin orbital (TB-LMTO) approach in the so-called most localized or β representation.[17] The choice of the β representation is dictated by our subsequent application to substitutionally disordered alloys where the disorder is *local* and a real-space formulation with a sparse Hamiltonian is most convenient. The Hamiltonian in this representation is given by

$$\mathcal{H}^{\beta} = \sum_{\vec{R}} \underline{\underline{C}}^{\beta}_{\vec{R}} \mathcal{P}_{\vec{R}} + \sum_{\vec{R}} \sum_{\vec{R}'} (\underline{\underline{\Delta}}^{\beta}_{\vec{R}})^{1/2} \underline{\underline{S}}^{\beta}_{\vec{R}\vec{R}'} (\underline{\underline{\Delta}}^{\beta}_{\vec{R}'})^{1/2} \mathcal{T}_{\vec{R}\vec{R}'}, \qquad (1)$$

where $\vec{R}$, and $\vec{R}'$ are the positions of the ion cores, the potential parameters are matrices in angular momentum $[L=(\ell m \sigma)]$ space, the operators $\mathcal{P}_{\vec{R}}=|\vec{R}\rangle\langle\vec{R}|$ and $\mathcal{T}_{\vec{R}\vec{R}'}=|\vec{R}\rangle\langle\vec{R}'|+|\vec{R}'\rangle\langle\vec{R}|$ are the projection and transfer operators on the space spanned by the muffin-tin orbital basis set $\{|\vec{R}\rangle\}$. The quantities $\underline{\underline{C}}^{\beta}_{\vec{R}}$ and $\underline{\underline{\Delta}}^{\beta}_{\vec{R}}$ are diagonal in angular momentum space and describe the positions and widths of the energy bands. The short-range structure matrix $\underline{\underline{S}}^{\beta}_{\vec{R}\vec{R}'}$ is dependent on the spatial arrangements of the muffin-tin potentials and in a substitutionally disordered alloy is usually nonrandom: $\underline{\underline{S}}^{\beta}_{\vec{R}\vec{R}}=\underline{\underline{S}}^{\beta}_{0}$ and $\underline{\underline{S}}^{\beta}_{\vec{R}\vec{R}'}=\underline{\underline{S}}^{\beta}(\vec{R}\text{-}\vec{R}')$. In what follows, the diagonal part $\underline{\underline{S}}^{\beta}_{0}$ has been incorporated within the diagonal potential parameter $\underline{\underline{C}}^{\beta}_{\vec{R}}$. If the constituents, however, have large differences in atomic size, there could be local lattice distortions which are significant and lead to off-diagonal disorder in the structure matrix.

The Green's function may now be written as

$$\underline{\underline{G}}_{\vec{R}\vec{R}'}(z) = \underline{\underline{\lambda}}^{\beta}_{\vec{R}}(z)\,\delta_{\vec{R}\vec{R}'} + \underline{\underline{\Delta}}^{\beta}_{\vec{R}}(z)^{-1/2} \underline{\underline{T}}^{\beta}_{\vec{R}\vec{R}'}(z) \underline{\underline{\Delta}}^{\beta}_{\vec{R}}(z)^{-1/2}, \qquad (2)$$

where

$$\mathcal{T}^{\beta}(z)^{-1} = \sum_{\vec{R}} \underline{\underline{P}}^{\beta}_{\vec{R}}(z)\mathcal{P}_{\vec{R}} - \sum_{\vec{R}} \sum_{\vec{R}'} \underline{\underline{S}}^{\beta}_{\vec{R}\text{-}\vec{R}'} \mathcal{T}_{\vec{R}\vec{R}'},$$

$$\underline{\underline{P}}^{\beta}_{\vec{R}}(z) = (\underline{\underline{\Delta}}^{\beta}_{\vec{R}})^{-1/2}(z\underline{\underline{I}} - \underline{\underline{C}}^{\beta}_{\vec{R}})(\underline{\underline{\Delta}}^{\beta}_{\vec{R}})^{-1/2},$$

$$\underline{\underline{\lambda}}^{\beta}_{\vec{R}}(z) = (\underline{\underline{\gamma}} - \underline{\underline{\beta}})(\underline{\underline{\Delta}}^{\gamma}_{\vec{R}})^{-1/2}(\underline{\underline{\Delta}}^{\beta}_{\vec{R}})^{1/2}. \qquad (3)$$

The values for the parameters $\beta_L=\beta_\ell$ for which we have maximum localization of the structure matrix were given by Andersen and Jepsen,[17] while the parameters γ_ℓ are obtained through the LMTO procedure together with the other potential parameters.

In the absence of off-diagonal disorder in the structure matrices, all random "potential parameters" in the Hamiltonian representation are *local* quantities, and this representation is ideal for the description of substitutional randomness. We associate with each $\vec{R}$ labeled member of the basis set a random "occupation" variable $n_{\vec{R}}$ such that

$$n_{\vec{R}} = \begin{cases} 1 & \text{if site } \vec{R} \text{ is occupied by an } A \text{ atom, with probability } y \\ 0 & \text{if site } \vec{R} \text{ is occupied by a } B \text{ atom, with probability } x = 1-y. \end{cases}$$

Putting this back into Eq. (2) and taking configuration averaging, we get

$$\begin{aligned} \langle\langle G_{\vec{R}L,\vec{R}L}\rangle\rangle = {} & \langle\langle \lambda^{\beta}_{\vec{R}L}\rangle\rangle + \mu_L^2(z)\langle\langle T^{\beta}_{\vec{R}L,\vec{R}L}(z)\rangle\rangle \\ & + \mu_L(z)\langle\langle T^{\beta}_{\vec{R}L,\vec{R}L}(z) n_{\vec{R}}\rangle\rangle \delta\mu_L(z) \\ & + \delta\mu_L(z)\langle\langle n_{\vec{R}} T^{\beta}_{\vec{R}L,\vec{R}L}(z)\rangle\rangle \mu_L(z) \\ & + \delta\mu_L(z)\langle\langle n_{\vec{R}} T^{\beta}_{\vec{R}L,\vec{R}L}(z) n_{\vec{R}}\rangle\rangle \delta\mu_L(z), \end{aligned} \qquad (4)$$

where $\delta\mu_L(z)=\Delta^{\beta}_{AL}(z)^{-1/2}-\Delta^{\beta}_{BL}(z)^{-1/2}$ and $\mu_L(z)=\Delta^{\beta}_{AL}(z)^{-1/2}$.

We shall now introduce the augmented-space formalism for configuration averaging. The ideas behind the approach have been described in great detail in a monograph.[18] Here we shall briefly introduce only those essential points which will enable us to describe the cluster coherent potential approximation:

(i) The augmented-space approach[19] replaces all the random variables $n_{\vec{R}}$ with operators $N_{\vec{R}}$ whose projected spectral density is the probability density of the variables $n_{\vec{R}}$. The eigenstates of $N_{\vec{R}}$ span the "configuration" space of $n_{\vec{R}}$.

(ii) We work in a new basis of representation: $|\emptyset_{\vec{R}}\rangle=\sqrt{y}|1_{\vec{R}}\rangle+\sqrt{x}|0_{\vec{R}}\rangle$, the average state, and $|\{1_{\vec{R}}\}\rangle=\sqrt{x}|1_{\vec{R}}\rangle-\sqrt{y}|0_{\vec{R}}\rangle$, which describes a fluctuation about the average state. These two states span the configuration space $\phi_{\vec{R}}$ of $n_{\vec{R}}$ (of rank 2).

(iii) The full configuration space of all the variables $\{n_{\vec{R}}\}$ is $\Phi=\Pi^{\otimes}_{\vec{R}}\phi_{\vec{R}}$ and the configuration states are labeled by the sequence of sites where we have a state $|1_{\vec{R}}\rangle$. For example, the configuration $\{0_{\vec{R}},1_{\vec{R}'},1_{\vec{R}''},0_{\vec{R}'''},\ldots\}$ is denoted by the sequence $\{\mathcal{C}\}\equiv\{\vec{R}',\vec{R}''\}$. This sequence is called the "cardinality" sequence and it uniquely labels a given configuration. In configuration space: $\langle\{\mathcal{C}\}|\{\mathcal{C}'\}\rangle=\delta(\mathcal{C},\mathcal{C}')$.

(iv) The operators in full configuration space corresponding to the binary random variables $\{n_{\vec{R}}\}$ $\Phi=\Pi^{\otimes}_{\vec{R}}\phi_{\vec{R}}$ are[20]

$$\hat{N}_{\vec{R}} = y\hat{\mathcal{P}}^{\emptyset}_{\vec{R}} + x\hat{\mathcal{P}}^{1}_{\vec{R}} + \sqrt{xy}\,\hat{\mathcal{T}}^{01}_{\vec{R}}. \tag{5}$$

Here, $\hat{\mathcal{P}}^{\lambda}_{\vec{R}}=I\otimes\cdots\otimes|\lambda_{\vec{R}}\rangle\langle\lambda_{\vec{R}}|\otimes\cdots$ and $\hat{\mathcal{T}}^{\lambda\lambda'}_{\vec{R}}=I\otimes\cdots\otimes(|\lambda_{\vec{R}}\rangle\langle\lambda'_{\vec{R}}|+|\lambda'_{\vec{R}}\rangle\langle\lambda_{\vec{R}}|)\otimes\cdots$, where $\lambda\neq\lambda'=\emptyset,1$. The projection operator counts the number of configuration fluctuations at the site $\vec{R}$, while the transfer operators create or annihilate configuration fluctuations at the site $\vec{R}$.

(v) Any random local potential parameter $X_{\vec{R}}$ in the Hamiltonian now can be expressed in terms of $n_{\vec{R}}$ as in Eq. (5). The augmented-space theorem replaces $n_{\vec{R}}$ with corresponding operator $\hat{N}_{\vec{R}}$, so $X_{\vec{R}}$ is replaced by an operator $\hat{X}_{\vec{R}}$ in the configuration space spanned by the configuration states of $N_{\vec{R}}$ and can be written as

$$\hat{X}_{\vec{R}} = A(X)\hat{\mathcal{P}}^{0}_{\vec{R}} + B(X)\hat{\mathcal{P}}^{1}_{\vec{R}} + F(X)\hat{\mathcal{T}}^{01}_{\vec{R}}, \tag{6}$$

where

$$A(X) = \langle\langle X\rangle\rangle = yX_A + xX_B,$$

$$B(X) = xX_A + yX_B,$$

$$F(X) = \sqrt{xy}(X_A - X_B). \tag{7}$$

(vi) The augmented-space theorem[19] tells us that the configuration average of any function of $\{n_{\vec{R}}\}$ is

$$\langle\langle f[H(\{n_{\vec{R}}\})]\rangle\rangle = \langle\{\emptyset\}|\hat{f}[\hat{H}(\{\hat{N}_{\vec{R}}\})]|\{\emptyset\}\rangle, \tag{8}$$

where $|\{\emptyset\}\rangle=\Pi^{\otimes}_{\vec{R}}|\{0_{\vec{R}}\}\rangle$.

(vii) Let us now apply the augmented-space theorem to the different averages quoted in Eq. (4):

$$\langle\langle T^{\beta}_{\vec{R}L,\vec{R}L}(z)\rangle\rangle = \langle\vec{R}L\otimes\{\emptyset\}|\tilde{\mathcal{T}}^{\beta}(z)|\vec{R}L\otimes\{\emptyset\}\rangle,$$

$$\begin{aligned}\langle\langle T^{\beta}_{\vec{R}L,\vec{R}L}(z)n_{\vec{R}}\rangle\rangle &= y\langle\vec{R}L\otimes\{\emptyset\}|\tilde{\mathcal{T}}^{\beta}(z)|\vec{R}L\otimes\{\emptyset\}\rangle\\ &\quad+\sqrt{xy}\langle\vec{R}L\otimes\{\emptyset\}|\tilde{\mathcal{T}}^{\beta}(z)|\vec{R}L\otimes\{\vec{R}\}\rangle,\end{aligned}$$

$$\begin{aligned}\langle\langle n_{\vec{R}}T^{\beta}_{\vec{R}L,\vec{R}L}(z)\rangle\rangle &= y\langle\vec{R}L\otimes\{\emptyset\}|\tilde{\mathcal{T}}^{\beta}(z)|\vec{R}L\otimes\{\emptyset\}\rangle\\ &\quad+\sqrt{xy}\langle\vec{R}L\otimes\{\vec{R}\}|\tilde{\mathcal{T}}^{\beta}(z)|\vec{R}L\otimes\{\emptyset\}\rangle,\end{aligned}$$

$$\begin{aligned}\langle\langle n_{\vec{R}}T^{\beta}_{\vec{R}L,\vec{R}L}(z)n_{\vec{R}}\rangle\rangle &= y^2\langle\vec{R}L\otimes\{\emptyset\}|\tilde{\mathcal{T}}^{\beta}(z)|\vec{R}L\otimes\{\emptyset\}\rangle\cdots\\ &\quad+y\sqrt{xy}[\langle\vec{R}L\otimes\{\emptyset\}|\tilde{\mathcal{T}}^{\beta}(z)|\vec{R}L\otimes\{\vec{R}\}\rangle\cdots\\ &\quad+\langle\vec{R}L\otimes\{\vec{R}\}|\tilde{\mathcal{T}}^{\beta}(z)|\vec{R}L\otimes\{\emptyset\}\rangle]\cdots\\ &\quad+xy\langle\vec{R}L\otimes\{\vec{R}\}|\tilde{\mathcal{T}}^{\beta}(z)|\vec{R}L\otimes\{\vec{R}\}\rangle,\end{aligned} \tag{9}$$

where

$$\begin{aligned}\tilde{\mathcal{T}}^{\beta}(z)^{-1} &= \sum_{\vec{R}} A(\underline{\underline{P}}^{\beta})\mathcal{P}_{\vec{R}}\otimes\hat{I}\cdots+\sum_{\vec{R}} B(\underline{\underline{P}}^{\beta})\mathcal{P}_{\vec{R}}\otimes\hat{\mathcal{P}}^{1}_{\vec{R}}\cdots\\ &\quad+\sum_{\vec{R}} F(\underline{\underline{P}}^{\beta})\mathcal{P}_{\vec{R}}\otimes\hat{\mathcal{T}}^{\emptyset 1}_{\vec{R}} - \sum_{\vec{R}}\sum_{\vec{R}'}\underline{\underline{S}}^{\beta}_{\vec{R}\text{-}\vec{R}''}\mathcal{T}_{\vec{R}\text{-}\vec{R}''}\otimes\hat{I}.\end{aligned} \tag{10}$$

The functions A, B, and F are defined in Eq. (7).

We shall make two comments here: first, it is important to note that the result quoted above is *exact*. Although the mathematical formulation is attractive, it is not very useful for actual calculations in specific real alloy systems since the dimension of the augmented space is essentially infinite and the representation of the operators are matrices of infinite rank. We need to introduce approximations which maintain the analytic and lattice translation properties of the configuration-averaged Green's functions. Several approximations have been proposed earlier. We shall discuss one such approximation in Sec. III and present it in a way that will allow us to use it as the basis for a calculation algorithm for real alloy systems.

The second comment is that the above formulation closely follows the Korringa-Kohn-Rostocker (KKR) method, which is the parent method of the LMTO. A KKR-CCPA formulation can therefore be stated exactly along the same lines. The correspondences are

$$P_{\vec{R}L}(z)\Rightarrow\tau^{-1}_{\vec{R}L}(z),\qquad S_{\vec{R}L,\vec{R}'L'}\Rightarrow -B_{\vec{R}L,\vec{R}'L'},$$

$$T_{\vec{R}L,\vec{R}'L'}(z)=\{[P(z)-S]^{-1}\}_{\vec{R}L,\vec{R}'L'}\Rightarrow\{[\tau^{-1}(z)+B]^{-1}\}_{\vec{R}L,\vec{R}'L'}.$$

III. CLUSTER COHERENT POTENTIAL APPROXIMATION

Self-consistent equations for the self-energies

We shall begin by the basic assumption of *all* mean-field theories: we suppose that there is a lattice translation symmetric effective system with a "Hamiltonian,"

$$\mathcal{T}^{\rm eff}(z) = H^{\rm eff}(z)^{-1} = \left[\sum_{\vec{R}}\underline{\underline{P}}^{\rm eff}(z)\mathcal{P}_{\vec{R}} - \sum_{\vec{R}}\sum_{\vec{R}'}\underline{\underline{S}}^{\rm eff}(\vec{R}\text{-}\vec{R}';z)\mathcal{T}_{RR'}\right]^{-1}, \tag{11}$$

such that

$$\langle\langle\underline{\underline{T}}^{\beta}_{\vec{R}\vec{R}'}(z)\rangle\rangle = \underline{\underline{T}}^{\rm eff}(\vec{R}\text{-}\vec{R}';z).$$

The problem to address then is the derivation of the effective medium terms $\underline{\underline{P}}^{\rm eff}(z)$ and $\underline{\underline{S}}^{\rm eff}(\vec{R}\text{-}\vec{R}';z)$.

To do this, let us first choose a site $\vec{R}_0$ with its cluster environment $\Xi_{\vec{R}_0}$ (see Fig. 1). In the full augmented space we choose the "augmented" cluster, that, is the cluster $\Xi_{\vec{R}_0}$ and all its possible configurations described by the cardinality sequences $\{\mathcal{C}(\Xi_{\vec{R}_0})\}$ of the type $\{\emptyset\}$ or $\{\vec{R}_1,\vec{R}_2,\ldots,\vec{R}_k\}$, where $1\leq k\leq n$ (the cluster size) and $\vec{R}_1,\vec{R}_2,\ldots\in\Xi_{\vec{R}_0}$. Let us call

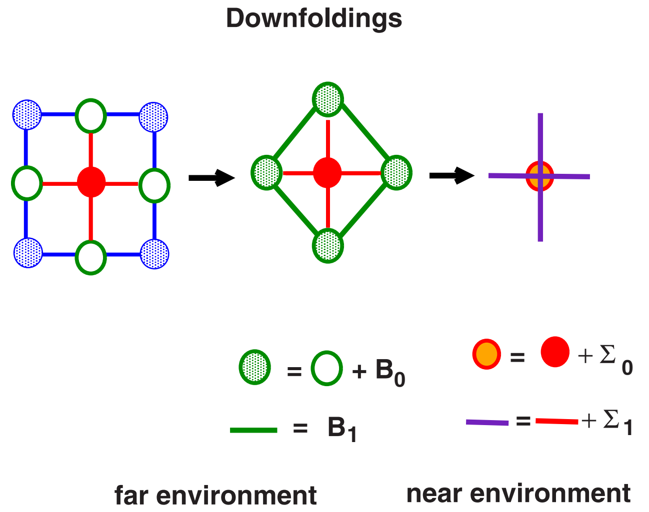

FIG. 1. (Color online) The downfoldings of the far and near environments. The cluster center is shown as red (black) circles, the near environment as green (white) circles, and the far environment as blue (gray) circles in the first term on the left. Successive downfoldings renormalize the Hamiltonian matrix elements.

the space spanned by $\Xi_{\vec{R}_0}\otimes\{\mathcal{C}(\Xi_{\vec{R}_0})\}$ as $\Psi_{\vec{R}_0}$. This is of rank $n\times 2^n$.

We shall now replace the entire remaining part of the lattice by the effective "medium" described in Eq. (11). The configuration space now reduces to the dimension 2^n of the configuration space of the cluster $\Xi_{\vec{R}_0}$ alone, spanned by states $\{\mathcal{C}(\Xi_{\vec{R}_0})\}$. In this *far* environment, outside the cluster, the configuration space collapses, as the effective medium is no longer random and there is just one configuration. We shall denote this collapsed augmented space by Ψ'. We shall partition the collapsed augmented space Ψ' into the space $\Psi_{\vec{R}_0}$ and the far environment ($\bar{\Psi}_{\vec{R}_0}=\Psi'\backslash\Psi_{\vec{R}_0}$).

The picture is now as follows: at the center of our system is the site $\vec{R}_0$ at which the occupations are random. In its immediate or *near* environment is made up of the rest of the sites of the cluster $\Xi_{\vec{R}_0}$. The Hamiltonian associated with the near environment is also random. Beyond that is the far environment which has been approximated by the nonrandom mean-field effective medium. If we now look at the Hamiltonian given in Eq. (10), we note that it remains invariant under the translation operator $\mathbf{T}_{\chi}$, where $\mathbf{T}_{\chi}|\vec{R},\{\vec{R}_1,\vec{R}_2,\ldots,\vec{R}_k\}\rangle = |\vec{R}+\chi,\{\vec{R}_1+\chi,\vec{R}_2+\chi,\ldots,\vec{R}_k+\chi\}\rangle$. Consequently it is immaterial where we choose the cluster center $\vec{R}_0$. We shall proceed to calculate the effect on the site $\vec{R}_0$ of its environment, both near and far. Since the procedure does not depend upon the choice of $\vec{R}_0$, its results for the configuration average should be lattice translationally invariant. This result is crucially dependent on the homogeneity of disorder. If the probability density $p(n_{\vec{R}})$ depended upon $\vec{R}$, the above statement would not be true.

The effects of the far and near environments are estimated through repeated downfoldings: first the far environment on the near environment and then the latter onto $\vec{R}_0$. The details of the mathematics can be obtained from Ref. 21. We shall quote here the main results.

The downfolding of the far environment leads to

$$\widetilde{\mathcal{T}}_0^{\beta}(z) = (\mathcal{A}_1-\mathcal{B})^{-\mathcal{P}_{\Psi_{\vec{R}_0}}},$$

$$\mathcal{A}_1 = \mathcal{P}_{\Psi_{\vec{R}_0}}[\widetilde{\mathcal{T}}_0^{\beta}(z)^{-1}]\mathcal{P}_{\Psi_{\vec{R}_0}}. \tag{12}$$

The effect of the far environment is contained in $\mathcal{B}$. If we define the self-energies as

$$\underline{\underline{P}}^{\mathrm{eff}}(z) = \langle\langle P^{\beta}\rangle\rangle + \underline{\underline{\Sigma}}_0(z),$$

$$\underline{\underline{S}}^{\mathrm{eff}}(\vec{R}-\vec{R}';z) = \underline{\underline{S}}^{\beta}(\vec{R}-\vec{R}') + \underline{\underline{\Sigma}}(\vec{R}-\vec{R}';z),$$

then it can be shown that

$$\mathcal{B}(\vec{k},z) = \underline{\underline{S}}^{\mathrm{eff}}(\vec{k},z)\underline{\underline{g}}(\vec{k},z)\underline{\underline{S}}^{\mathrm{eff}}(\vec{k},z), \tag{13}$$

where

$$\underline{\underline{g}}(\vec{k},z) = \underline{\underline{T}}^{\mathrm{eff}}(\vec{k},z)[\underline{\underline{I}}+\underline{\underline{\Delta}}(\vec{k},z)\underline{\underline{T}}^{\mathrm{eff}}(\vec{k},z)]^{-1}$$

and

$$\underline{\underline{\Delta}}(\vec{k},z) = \underline{\underline{\Sigma}}_0(z) + \underline{\underline{\Sigma}}(\vec{k},z).$$

It is obvious from Eq. (13) that the matrix elements of $\mathcal{B}$ are themselves functionals of $\underline{\underline{P}}^{\mathrm{eff}}$ and $\underline{\underline{S}}^{\mathrm{eff}}$:

$$\mathcal{B} = \sum_{R\in\Xi_{R_0}} \underline{\underline{B}}_0[\underline{\underline{P}}^{\mathrm{eff}}(z);\underline{\underline{S}}^{\mathrm{eff}}(z)]\mathcal{P}_{\vec{R}}\cdots$$

$$-\sum_{R,R'\in\Xi_{R_0}} \underline{\underline{B}}(R\text{-}R';\underline{\underline{P}}^{\mathrm{eff}}(z);\underline{\underline{S}}^{\mathrm{eff}}(z))\mathcal{T}_{\vec{R}\vec{R}'}$$

and

$$\underline{\underline{T}}^{\mathrm{eff}}(\vec{R}\text{-}\vec{R}';z) = \int \frac{d^3\vec{k}}{8\pi^3}e^{i\vec{k}\cdot(\vec{R}\text{-}\vec{R}')}[\underline{\underline{P}}^{\mathrm{eff}}(z)-\underline{\underline{S}}^{\mathrm{eff}}(\vec{k},z)]^{-1},$$

$$\underline{\underline{B}}(\vec{R}\text{-}\vec{R}';z) = \int \frac{d^3\vec{k}}{8\pi^3}e^{i\vec{k}\cdot(\vec{R}\text{-}\vec{R}')}\underline{\underline{B}}(\vec{k};z). \tag{14}$$

Having downfolded the effect of the far environment on to the cluster chosen, the augmented space has been reduced to Ψ_0 of rank $n\times 2^n$, where n is the size of $\Xi_{\vec{R}_0}$. The next step would be to partition Ψ_0 to a space Φ of rank n, spanned by the states $|\vec{R}\in\Xi_{\vec{R}_0}\otimes\emptyset\rangle$ and its complement $\bar{\Phi}$ in Ψ_0:

$$\widetilde{\mathcal{T}}_0 = \begin{pmatrix} \mathcal{D}_1 & \mathcal{D}' \\ \mathcal{D}^T & \mathcal{D}_2 \end{pmatrix}.$$

The downfolding theorem gives

$$\mathcal{D}_1^{-\mathcal{P}_{\Phi}} = (\mathcal{D}_1-\mathcal{D}'\mathcal{D}_2^{-\mathcal{P}_{\bar{\Phi}}}\mathcal{D}'^{T})^{-\mathcal{P}_{\Phi}}. \tag{15}$$

We now are working in the vastly reduced augmented space of dimension m. All inverses will now refer to this m-dimensional Hilbert space.

Again, with a little mathematics (details of which can be accessed from Ref. 21), we obtain the self-consistency equations for the self-energies:

$$\underline{\underline{\Sigma}}_0(z) = \underline{\underline{B}}_0(z) + \langle\vec{R}\|\mathcal{K}\|\vec{R}\rangle,$$

$$\underline{\underline{\Sigma}}(\vec{R}\text{-}\vec{R}';z) = \underline{\underline{B}}(\vec{R}\text{-}\vec{R}';z) + \langle \vec{R} \| \mathcal{K} \| \vec{R}' \rangle, \tag{16}$$

where $\vec{R},\vec{R}' \in \Xi_{\vec{R}_0}$, $\mathcal{D}_2^{-\mathcal{P}\bar{\Phi}} = \mathcal{K}$, and

$$\langle \vec{R} \| = \sum_{\vec{R}'' \neq \Xi_{\vec{R}_0}} \underline{\underline{\sigma}}(\vec{R}\text{-}\vec{R}'';z)\langle \vec{R}'' \otimes \{\emptyset\}| + \cdots + F(\underline{\underline{P}}^{\beta})\langle \vec{R} \otimes \{\vec{R}\}|,$$

$$\underline{\underline{\sigma}}(\vec{R}\text{-}\vec{R}';z) = \underline{\underline{S}}^{\beta}(\vec{R}\text{-}\vec{R}') - \underline{\underline{B}}(\vec{R}\text{-}\vec{R}';z).$$

The matrix elements in Eq. (16) are written in terms of the matrix elements of $\mathcal{K}$:

$$\langle \vec{R}_p \otimes \{\emptyset\}|\mathcal{K}|\vec{R}_{p'} \otimes \{\emptyset\}\rangle, \quad \langle \vec{R} \otimes \{\emptyset\}|\mathcal{K}|\vec{R}_p \otimes \{\vec{R}_p\}\rangle,$$

and

$$\langle \vec{R}_p \otimes \{\vec{R}_p\}|\mathcal{K}|\vec{R}_{p'} \otimes \{\vec{R}_{p'}\}\rangle, \quad \text{where } p,p' = 0,1.$$

Since the subspace $\bar{\Phi}$ of the full augmented space is of finite rank, these matrix elements of $\mathcal{K}$ can be obtained by a simple matrix inversion of $\mathcal{D}_2$ in this subspace. The two downfolding procedures are best illustrated by the schematic in Fig. 1 shown here.

These are the equations for the CCPA self-energies. We again emphasize that the choice of $\vec{R}_0$ is immaterial, and in the absence of anisotropy in the Hamiltonian, so is the choice of $\vec{R}_1$. The effective medium off-diagonal matrix element in the direction of $\vec{R}_2 - \vec{R}_0$ is related to that in the direction $\vec{R}_1 - \vec{R}_0$ by a rotation matrix:

$$\underline{\underline{S}}^{\mathrm{eff}}(\vec{R}_0 - \vec{R}_2;z) = \underline{\underline{U}}^{T}\underline{\underline{S}}^{\mathrm{eff}}(\vec{R}_0 - \vec{R}_1;z)\underline{\underline{U}}.$$

Finally, we need to calculate the other average terms in Eqs. (4) and (9). For this we partition the $\tilde{\mathcal{T}}_0^{\beta}$ into a subspace π of rank 1, spanned by the state $|\vec{R}_0 \otimes \emptyset\rangle$ and its complement $\bar{\pi}$ in Ψ_0:

$$\tilde{\Gamma}_0 = \left(\begin{array}{c|c} \mathcal{E}_1 & \mathcal{E}' \\ \hline \mathcal{E}'^{T} & \mathcal{E}_2 \end{array}\right).$$

Downfolding and taking appropriate matrix elements (see Ref. 21), we get

$$\begin{aligned}
&\langle \vec{R}_0 \otimes \{\emptyset\}|\underline{\underline{\mathcal{T}}}^{\beta}|\vec{R}_0 \otimes \{\vec{R}_0\}\rangle \\
&\quad = \langle\langle \underline{\underline{T}}^{\beta}_{\vec{R}_0,\vec{R}_0}\rangle\rangle \left[F(\underline{\underline{P}}^{\beta})\underline{\underline{\Gamma}}^{(2)}_{\vec{R}_0,\vec{R}_0} + \sum_{\vec{R} \neq \vec{R}_0} \underline{\underline{\sigma}}(\vec{R}_0\text{-}\vec{R};z)\underline{\underline{\Gamma}}^{(1)}_{\vec{R},\vec{R}_0} \right] \\
&\quad = \langle\langle \underline{\underline{T}}^{\beta}_{\vec{R}_0,\vec{R}_0}\rangle\rangle \underline{\underline{W}}_{\vec{R}_0,\vec{R}_0},
\end{aligned}$$

$$\langle \vec{R}_0 \otimes \{\vec{R}_0\}|\underline{\underline{\mathcal{T}}}^{\beta}|\vec{R}_0 \otimes \{\emptyset\}\rangle = \underline{\underline{W}}_{\vec{R}_0,\vec{R}_0}\langle\langle \underline{\underline{T}}^{\beta}_{\vec{R}_0,\vec{R}_0}\rangle\rangle,$$

$$\langle \vec{R}_0 \otimes \{\vec{R}_0\}|\underline{\underline{\mathcal{T}}}^{\beta}|\vec{R}_0 \otimes \{\vec{R}_0\}\rangle = \underline{\underline{\Gamma}}^{(2)}_{\vec{R}_0,\vec{R}_0} + \underline{\underline{W}}_{\vec{R}_0,\vec{R}_0}\langle\langle \underline{\underline{T}}^{\beta}_{\vec{R}_0,\vec{R}_0}\rangle\rangle \underline{\underline{W}}_{\vec{R}_0,\vec{R}_0}, \tag{17}$$

where

$$\underline{\underline{\Gamma}}^{(2)}_{\vec{R}_0,\vec{R}_0} = \langle \vec{R}_0 \otimes \{\vec{R}_0\}|\underline{\underline{\mathcal{E}}}_2^{-\mathcal{P}\bar{\pi}}|\vec{R}_0 \otimes \{\vec{R}_0\}\rangle,$$

$$\underline{\underline{\Gamma}}^{(2)}_{\vec{R},\vec{R}_0} = \langle \vec{R} \otimes \{\emptyset\}|\underline{\underline{\mathcal{E}}}_2^{-\mathcal{P}\bar{\pi}}|\vec{R}_0 \otimes \{\vec{R}_0\}\rangle.$$

Now substituting in Eqs. (4) and (9), we get

$$\langle\langle \underline{\underline{G}}_{\vec{R}_0\vec{R}_0}\rangle\rangle = \langle\langle \underline{\underline{\lambda}}_{\vec{R}_0}\rangle\rangle + \underline{\underline{\mu}}^{\mathrm{eff}}_{\vec{R}_0}\langle\langle \underline{\underline{T}}^{\beta}_{\vec{R}_0\vec{R}_0}\rangle\rangle \underline{\underline{\mu}}^{\mathrm{eff}}_{\vec{R}_0} + \underline{\underline{\delta\mu}}\,\underline{\underline{\Gamma}}^{(2)}_{\vec{R}_0\vec{R}_0}\underline{\underline{\delta\mu}},$$

where

$$\underline{\underline{\mu}}^{\mathrm{eff}}_{\vec{R}_0} = \langle\langle \underline{\underline{\mu}}\rangle\rangle + \sqrt{xy}\,\underline{\underline{\delta\mu}}\,\underline{\underline{W}}_{\vec{R}_0\vec{R}_0}. \tag{18}$$

IV. CONFIGURATION-AVERAGED SPECTRAL FUNCTIONS AND COMPLEX BAND STRUCTURES

Going back to Eqs. (2) and (18), we note the following: homogeneity of disorder leads to $\underline{\underline{\mu}}^{\mathrm{eff}}_{\vec{R}_0} = \underline{\underline{\mu}}^{\mathrm{eff}} = \langle\langle \underline{\underline{\mu}}\rangle\rangle + \sqrt{xy}\,\underline{\underline{\delta\mu}}\,\underline{\underline{W}}$ and

$$\langle\langle \underline{\underline{G}}(R_0\text{-}R_1;z)\rangle\rangle = \underline{\underline{\mu}}^{\mathrm{eff}}(z)\langle\langle \underline{\underline{T}}^{\beta}(R_0\text{-}R_1;z)\rangle\rangle \underline{\underline{\mu}}^{\mathrm{eff}}(z).$$

Spatial homogeneity gives

$$\langle\langle \underline{\underline{G}}(\vec{k};z)\rangle\rangle = \underline{\underline{\mu}}^{\mathrm{eff}}(z)\langle\langle \underline{\underline{T}}^{\beta}(\vec{k};z)\rangle\rangle \underline{\underline{\mu}}^{\mathrm{eff}}(z), \tag{19}$$

where

$$\langle\langle \underline{\underline{T}}^{\beta}(\vec{k};z)\rangle\rangle = [\langle\langle \underline{\underline{P}}^{\beta}\rangle\rangle - \underline{\underline{S}}^{\beta}(\vec{k}) + \underline{\underline{\Sigma}}_0(z) - \underline{\underline{\Sigma}}(\vec{k};z)]^{-1}. \tag{20}$$

The self-energy in reciprocal space may be obtained from Eq. (16) by Fourier transformation:

$$\underline{\underline{\Sigma}}(\vec{k};z) = \sum_{\vec{\chi}} \underline{\underline{\Sigma}}(\vec{\chi};z)\exp(i\vec{k}\cdot\vec{\chi}), \tag{21}$$

where $\vec{\chi}$ are the vectors joining any two sites in the cluster. We should note that although the Hamiltonian may have only nearest-neighbor matrix elements, because of downfolding of the far environment, the self-energies, in general, connect all sites of the cluster.

The configuration-averaged spectral function is given by

$$\langle\langle A(\vec{k},E)\rangle\rangle = -\frac{1}{\pi}\lim_{\delta\to 0}\,\mathrm{Im}\,\mathrm{Tr}\langle\langle \underline{\underline{G}}(\vec{k};E+i\delta)\rangle\rangle. \tag{22}$$

Unlike the periodic solid where the spectral function is a bunch of delta functions at the eigenvalues of the periodic Hamiltonian, for disordered systems aperiodicity in the potential leads to scattering of the Bloch-type functions. Consequently the complex self-energy gives both a shift and a Lorenzian width to the delta functions.

The complex band structure of random systems is obtained directly from the spectral functions. For ordered materials for a given $\vec{k}$ the spectral function $A(\vec{k},E)$ is a bunch of delta functions at $E=E(\vec{k})$. For disordered materials the configuration-averaged spectral functions have peaks at $E(\vec{k})$ which locate the position of the bands. If we fit Lorenzians around these peaks, the half-widths will measure the spread or "fuzziness" of the bands. This has been plotted in Fig. 3. We should note that the spectral function near a peak may have considerable asymmetry. In such cases we really cannot fit it to a Lorenzian near the peak. This description becomes inaccurate in those circumstances.

V. COMMENTS

We stress again that the downfolding approach here differs significantly from the earlier proposed cluster coherent potential approximations. We do not begin by partitioning the Hilbert space into clusters. There were always objections that the procedure was not unique and the results violated the translation symmetry of averaged quantities: replacing it by a cluster translational symmetry. Rather, our approach focuses on any site and estimates the effect of configuration fluctuations of its environment on the local properties at that point, using a downfolding technique. In the augmented space, if the disorder is homogeneous, the environment of every site is identical. Thus our choice of the central site is immaterial and the formulation maintains the lattice translational symmetry of configuration-averaged quantities. In case the system has more than one atom per unit cell, we can generalize our ideas concentrating on a unit cell (instead of a site) and estimating the effect of configuration fluctuations of the environment of the cell by the downfolding technique.

We distinguish both the immediate or near environment (and retain its randomness *exactly*) and the far environment, which we approximate by an effective medium. We go on to obtain this effective medium self-consistently using successive downfoldings. Razee and Prasad[3] showed that if we consider the entire environment of a site as an effective far environment, we recover the single-site CPA. In that sense the formulation is a generalization of the CPA.

In a formal paper Razee *et al.*[22] showed that the downfolding generalization retains the Herglotz analytic properties of the approximated averaged Green's function. This is an essential property of any successful generalization of the CPA.

The CCPA proposed here is closely related to the TB-LMTO-ASR,[23,24] which is based on the recursion method.[25] It is known that the recursion method successively partitions the full augmented space into subspaces which are successively the further and further shell environments of the starting site. The continued fraction expansion of the Green's function is generated by repeated downfolding using successive applications of the partitioning theorem. In the TB-LMTO-ASR the near environment is the number of recursion steps one carries out *exactly* and the far environment is estimated approximately through the *terminator*.[26] In our present formulation, the far environment is estimated in a more transparent self-consistent mean-field approach. The formulation also has close affinities with the itinerant cluster coherent potential (ICPA) proposed by Ghosh *et al.*[4] Since the idea of approximation is very similar, it would be interesting to work out an exact relationship between the two. Similarities with the traveling cluster approximation (TCA) of Mills and co-workers[27,28] are also apparent, although the TCA approached the problem using a multiple-scattering approach. For the CPA, the mean-field and the multiple-scattering approaches give identical results. It would be interesting to examine whether this is true also for this CCPA and the TCA. We propose to examine these relationships in a subsequent paper.

VI. SHORT-RANGE ORDER

In Sec. V we have described a CCPA approach based on the augmented-space formalism for substitutional alloys whose occupation probabilities are homogeneously and independently distributed. However, most disordered alloys have a certain degree of short-range order (SRO) dictated by the local chemistry of the constituents. Such SRO cannot be described by single-site mean-field approximations. On the other hand, the approach suggested by us, where the effect of the environment of any chosen site is estimated by a downfolding procedure, is ideal for such a description. Short-range order is described by correlated distribution of the site occupation variable of any chosen site with those of its near environment. In an earlier paper Mookerjee and Prasad[29] generalized the augmented-space formalism to include such SRO. In the downfolding procedure, to obtain the self-consistent equations for the self-energies, we had partitioned the augmented space into one spanned by $|\vec{R}_0 \otimes \emptyset\rangle$ and $|\vec{R}_0 \otimes \{\vec{R}_0\}\rangle$. We shall do this again, but this time the augmented-space operator $\hat{N}_{\vec{R}_0}$ given in Eq. (5) will be replaced by Eq. (17) of Mookerjee and Prasad:[29]

$$
\begin{aligned}
\hat{N}_{\vec{R}_0} = y\hat{I} + (x-y)\hat{\mathcal{P}}^{01}_{\vec{R}_0\vec{R}_1} + (X-y)\hat{\mathcal{P}}^{10}_{\vec{R}_0\vec{R}_1} + (X'-y)\hat{\mathcal{P}}^{11}_{\vec{R}_0\vec{R}_1} \\
+ B_1\hat{\mathcal{Q}}^{0,01}_{\vec{R}_0\vec{R}_1} + B_2\hat{\mathcal{Q}}^{1,01}_{\vec{R}_0\vec{R}_1} + B_3\hat{\mathcal{Q}}'^{01,0}_{\vec{R}_0\vec{R}_1} \\
+ B_4\hat{\mathcal{Q}}'^{01,1}_{\vec{R}_0\vec{R}_1} + B_5\hat{R}^{01,01}_{\vec{R}_0\vec{R}_1},
\end{aligned}
\tag{23}
$$

where

$$
\hat{\mathcal{P}}^{\lambda\lambda'}_{\vec{R}_0\vec{R}_1} = I \otimes \cdots \mathcal{P}^{\lambda}_{\vec{R}_0} \otimes \cdots \mathcal{P}^{\lambda'}_{\vec{R}_1} \otimes \cdots,
$$

$$
\hat{\mathcal{Q}}^{\lambda,\lambda'\lambda''}_{\vec{R}_0\vec{R}_1} = I \otimes \cdots \mathcal{P}^{\lambda}_{\vec{R}_0} \otimes \cdots \mathcal{T}^{\lambda',\lambda''}_{\vec{R}_1} \otimes \cdots,
$$

$$
\hat{\mathcal{Q}}^{\lambda'\lambda'',\lambda}_{\vec{R}_0\vec{R}_1} = I \otimes \cdots \mathcal{T}^{\lambda'\lambda''}_{\vec{R}_0} \otimes \cdots \mathcal{P}^{\lambda}_{\vec{R}_1} \otimes \cdots,
$$

$$
\hat{\mathcal{R}}^{\lambda\lambda',\lambda\lambda'}_{\vec{R}_0\vec{R}_1} = I \otimes \cdots \mathcal{T}^{\lambda,\lambda'}_{\vec{R}_0} \otimes \cdots \mathcal{T}^{\lambda\lambda'}_{\vec{R}_1} \otimes \cdots,
$$

where $\lambda, \lambda', \lambda'' = 0, 1$ and

$$
X = y - \alpha(y-x), \quad X' = x + \alpha(y-x),
$$

$$
B_1 = y\sqrt{(1-\alpha)x(y+\alpha x)} + x\sqrt{(1-\alpha)y(x+\alpha y)},
$$

$$
B_2 = x\sqrt{(1-\alpha)x(y+\alpha x)} + y\sqrt{(1-\alpha)y(x+\alpha y)},
$$

$$
B_3 = \alpha\sqrt{xy} = -B_4,
$$

$$
B_5 = \sqrt{xy}[\sqrt{(1-\alpha)x(y+\alpha x)} - \sqrt{(1-\alpha)y(x+\alpha y)}].
$$

The rest of the downfolding procedure follows exactly as before and leads to the self-consistency equations

$$
\underline{\underline{\Sigma}}_{\vec{R}_0}(z) = \underline{\underline{B}}_0(z) + \langle \vec{R}_0 \| \mathcal{K} \| \vec{R}_0 \rangle,
$$

$$
\underline{\underline{\Sigma}}(\vec{R}_0\text{-}\vec{R}_1; z) = \underline{\underline{B}}(\vec{R}_0\text{-}\vec{R}_1; z) + \langle \vec{R}_0 \| \mathcal{K} \| \vec{R}_1 \rangle,
\tag{24}
$$

where

$$\begin{aligned}\langle \vec{R}_0 \| = \sum_{\vec{R}'' \neq \Xi_{\vec{R}_0}} & \underline{\underline{\sigma}}(\vec{R}_0\text{-}\vec{R}'';z)\langle \vec{R} \otimes \{\emptyset\}| \\ & + F_1(\underline{\underline{P}}^{\beta})\langle \vec{R}_0 \otimes \{\vec{R}_0\}| + F_2(\underline{\underline{P}}^{\beta})\langle \vec{R}_0 \otimes \{\vec{R}_1\}| \\ & + F_3(\langle\langle \underline{\underline{P}}^{\beta}\rangle\rangle)\langle \vec{R}_0 \otimes \{\vec{R}_0\vec{R}_1\}|,\end{aligned}$$

$$\langle \vec{R}_1 \| = \sum_{\vec{R} \neq \Xi_{\vec{R}_0}} \underline{\underline{\sigma}}(\vec{R}_1\text{-}\vec{R};z)\langle \vec{R} \otimes \{\emptyset\}| + F(\underline{\underline{P}}^{\beta})\langle \vec{R}_1 \otimes \{\vec{R}_1\}|,$$

where

$$F_1(\underline{\underline{P}}^{\beta}) = B_4(\underline{\underline{P}}^{\beta}_A - \underline{\underline{P}}^{\beta}_B), \quad F_2(\underline{\underline{P}}^{\beta}) = B_2(\underline{\underline{P}}^{\beta}_A - \underline{\underline{P}}^{\beta}_B)$$

$$F_3(\underline{\underline{P}}^{\beta}) = B_5(\underline{\underline{P}}^{\beta}_A - \underline{\underline{P}}^{\beta}_B), \quad F(\underline{\underline{P}}^{\beta}) = \sqrt{xy}(\underline{\underline{P}}^{\beta}_A - \underline{\underline{P}}^{\beta}_B\underline{\underline{P}}^{\beta}_B).$$

Equation (24) then replaces the earlier Eq. (16). It is clear that the SRO affects the self-consistent far environment through the self-consistency equations. Our approach is thus superior to some earlier approaches where the cluster with SRO was immersed in a single-site CPA medium.

Finally the expression for $\underline{\underline{W}}_{\vec{R}_0\vec{R}_0}$ is replaced by

$$\begin{aligned}\underline{\underline{W}}_{\vec{R}_0\vec{R}_0} = {} & F_1(\underline{\underline{P}}^{\beta})\underline{\underline{\Gamma}}^{(2)}_{\vec{R}_0\vec{R}_0} + F_2(\underline{\underline{P}}^{\beta})\underline{\underline{\Gamma}}^{(3)}_{\vec{R}_0\vec{R}_0} + \cdots + F_3(\underline{\underline{P}}^{\beta})\underline{\underline{\Gamma}}^{(4)}_{\vec{R}_0\vec{R}_0} \\ & + \sum_{\vec{R} \neq \vec{R}_0} \underline{\underline{\sigma}}(\vec{R}_0\text{-}\vec{R};z)\underline{\underline{\Gamma}}^{(1)}_{\vec{R}\vec{R}_0},\end{aligned} \tag{25}$$

where the new matrix elements of $\underline{\underline{\mathcal{E}}}_2^{-\mathcal{P}_\pi}$ are

$$\underline{\underline{\Gamma}}^{(3)}_{\vec{R}_0\vec{R}_0} = \langle \vec{R}_0 \otimes \{\vec{R}_1\}|\underline{\underline{\mathcal{E}}}_2^{-\mathcal{P}_\pi}|\vec{R}_0 \otimes \{\vec{R}_0\}\rangle,$$

$$\underline{\underline{\Gamma}}^{(4)}_{\vec{R}_0\vec{R}_0} = \langle \vec{R}_0 \otimes \{\vec{R}_0\vec{R}_1\}|\underline{\underline{\mathcal{E}}}_2^{-\mathcal{P}_\pi}|\vec{R}_0 \otimes \{\vec{R}_0\}\rangle.$$

With these changes, the CCPA can self-consistently include the effects of SRO in its calculation of the averaged Green's functions.

VII. OFF-DIAGONAL DISORDER

In a substitutional alloy with local lattice distortions, the random off-diagonal structure matrices $\underline{\underline{S}}^{\beta}_{\vec{R}\vec{R}'}$ between the sites $\vec{R}$ and $\vec{R}'$ can be written, within the end-point approximation, in terms of the site occupation numbers $\{n_{\vec{R}}\}$ as

$$\begin{aligned}\underline{\underline{S}}^{\beta}_{\vec{R}\vec{R}'} = {} & \underline{\underline{S}}^{\beta}_{BB}(\vec{R}\text{-}\vec{R}') + [\underline{\underline{S}}^{\beta}_{AA}(\vec{R}\text{-}\vec{R}') + \underline{\underline{S}}^{\beta}_{BB}(\vec{R}\text{-}\vec{R}') \cdots \\ & - 2\underline{\underline{S}}^{\beta}_{AB}(\vec{R}\text{-}\vec{R}')]n_{\vec{R}}n_{\vec{R}'} + [\underline{\underline{S}}^{\beta}_{AB}(\vec{R}\text{-}\vec{R}') \cdots \\ & - \underline{\underline{S}}^{\beta}_{BB}(\vec{R}\text{-}\vec{R}')](n_{\vec{R}} + n_{\vec{R}'}).\end{aligned} \tag{26}$$

The downfolding procedure now follows exactly as before (details again are to be found in Ref. 21). We shall quote here the final equations for the self-energies:

$$\underline{\underline{\Sigma}}_0(z) = \underline{\underline{\Sigma}}_{\vec{R}_0}(z) + \langle \vec{R}_0 \| \mathcal{K} \| \vec{R}_0\rangle,$$

$$\underline{\underline{\Sigma}}(\vec{R}_0\text{-}\vec{R}_1;z) = \underline{\underline{B}}(\vec{R}_0\text{-}\vec{R}_1;z) + \langle \vec{R}_0 \| \mathcal{K} \| \vec{R}_1\rangle, \tag{27}$$

where

$$\begin{aligned}\langle \vec{R}_0 \| = {} & \underline{\underline{S}}^{(2)}(R_0\text{-}R_1)\langle \vec{R}_1 \otimes \{\vec{R}_0\}| + \underline{\underline{S}}^{(2)}(R_0\text{-}R_1)\langle \vec{R}_1 \otimes \{R_1\}| \cdots \\ & + \underline{\underline{S}}^{(5)}(R_0\text{-}R_1)\langle \vec{R}_1 \otimes \{\vec{R}_0\vec{R}_1\}| \cdots \\ & + \sum_{\vec{R} \neq \vec{R}_0\vec{R}_1} \underline{\underline{\sigma}}(\vec{R}_0\text{-}\vec{R};z)\langle \vec{R} \otimes \{\emptyset\}| \cdots + F(\underline{\underline{P}}^{\beta})\langle \vec{R}_0 \otimes \{\vec{R}_0\}|,\end{aligned}$$

$$\begin{aligned}\langle \vec{R}_1 \| = {} & \underline{\underline{S}}^{(2)}(R_0\text{-}R_1)\langle \vec{R}_0 \otimes \{\vec{R}_1\}| + \underline{\underline{S}}^{(2)}(R_0\text{-}R_1)\langle \vec{R}_0 \otimes \{\vec{R}_0\}| \\ & + \underline{\underline{S}}^{(5)}(R_0\text{-}R_1)\langle \vec{R}_0 \otimes \{\vec{R}_0\vec{R}_1\}| \\ & + \sum_{\vec{R} \neq \vec{R}_1\vec{R}_0} \underline{\underline{\sigma}}(\vec{R}_1\text{-}\vec{R};z)\langle \vec{R} \otimes \{\emptyset\}| + F(\underline{\underline{P}}^{\beta})\langle \vec{R}_1 \otimes \{\vec{R}_1\}|,\end{aligned}$$

where

$$\underline{\underline{S}}^{(1)}(\vec{R}\text{-}\vec{R}') = (x-y)\underline{\underline{\Phi}}^{(1)}(\vec{R}\text{-}\vec{R}'),$$

$$\underline{\underline{S}}^{(2)}(\vec{R}\text{-}\vec{R}') = \sqrt{xy}\underline{\underline{\Phi}}^{(1)}(\vec{R}\text{-}\vec{R}'),$$

$$\underline{\underline{S}}^{(3)}(\vec{R}\text{-}\vec{R}') = (x-y)^2\underline{\underline{\Phi}}^{(2)}(\vec{R}\text{-}\vec{R}'),$$

$$\underline{\underline{S}}^{(4)}(\vec{R}\text{-}\vec{R}') = \sqrt{xy}(x-y)\underline{\underline{\Phi}}^{(2)}(\vec{R}\text{-}\vec{R}'),$$

$$\underline{\underline{S}}^{(5)}(\vec{R}\text{-}\vec{R}') = xy\underline{\underline{\Phi}}^{(2)}(\vec{R}\text{-}\vec{R}'),$$

and

$$\begin{aligned}\underline{\underline{\Phi}}^{(1)}(\vec{R}\text{-}\vec{R}') = {} & y\underline{\underline{S}}^{\beta}_{AA}(\vec{R}\text{-}\vec{R}') - x\underline{\underline{S}}^{\beta}_{BB}(\vec{R}\text{-}\vec{R}') + \cdots \\ & + (x-y)\underline{\underline{S}}^{\beta}_{AB}(\vec{R}\text{-}\vec{R}'),\end{aligned}$$

$$\underline{\underline{\Phi}}^{(2)}(\vec{R}\text{-}\vec{R}') = \underline{\underline{S}}^{\beta}_{AA}(\vec{R}\text{-}\vec{R}') + \underline{\underline{S}}^{\beta}_{BB}(\vec{R}\text{-}\vec{R}') - 2\underline{\underline{S}}^{\beta}_{AB}(\vec{R}\text{-}\vec{R}').$$

Following the exact similar steps, the new expression for $\underline{\underline{W}}_{\vec{R}_0\vec{R}_0}$ becomes

$$\begin{aligned}\underline{\underline{W}}_{\vec{R}_0\vec{R}_0} = \Bigg[& F(\underline{\underline{P}}^{\beta})\underline{\underline{\Gamma}}^{(2)}_{\vec{R}_0,\vec{R}_0} + \sum_{\vec{R} \neq \vec{R}_0} \underline{\underline{\sigma}}(\vec{R}_0\text{-}\vec{R};z)\underline{\underline{\Gamma}}^{(1)}_{\vec{R},\vec{R}_0} \\ & + \underline{\underline{S}}^{(2)}(R_0\text{-}R_1)\underline{\underline{\Gamma}}^{(5)}_{\vec{R}_1\vec{R}_0} + \underline{\underline{S}}^{(2)}(R_0\text{-}R_1)\underline{\underline{\Gamma}}^{(6)}_{\vec{R}_1\vec{R}_0} \\ & + \underline{\underline{S}}^{(5)}(R_0\text{-}R_1)\underline{\underline{\Gamma}}^{(7)}_{\vec{R}_1\vec{R}_0}\Bigg],\end{aligned} \tag{28}$$

where

$$\underline{\underline{\Gamma}}^{(5)}_{\vec{R}_1\vec{R}_0} = \langle \vec{R}_1 \otimes \{\vec{R}_0\}|\underline{\underline{\mathcal{E}}}^{-\mathcal{P}_{\bar{\pi}}}|\vec{R}_0 \otimes \{\vec{R}_0\}\rangle,$$

$$\underline{\underline{\Gamma}}^{(6)}_{\vec{R}_1\vec{R}_0} = \langle \vec{R}_1 \otimes \{\vec{R}_1\}|\underline{\underline{\mathcal{E}}}^{-\mathcal{P}_{\bar{\pi}}}|\vec{R}_0 \otimes \{\vec{R}_0\}\rangle,$$

$$\underline{\underline{\Gamma}}^{(7)}_{\vec{R}_1\vec{R}_0} = \langle \vec{R}_1 \otimes \{\vec{R}_0\vec{R}_1\}|\underline{\underline{\mathcal{E}}}^{-\mathcal{P}_{\bar{\pi}}}|\vec{R}_0 \otimes \{\vec{R}_0\}\rangle.$$

VIII. APPLICATION TO THE EQUIATOMIC CuZn ALLOY

As an application of the above methodology, we shall study the electronic structure of the equiatomic CuZn alloy.

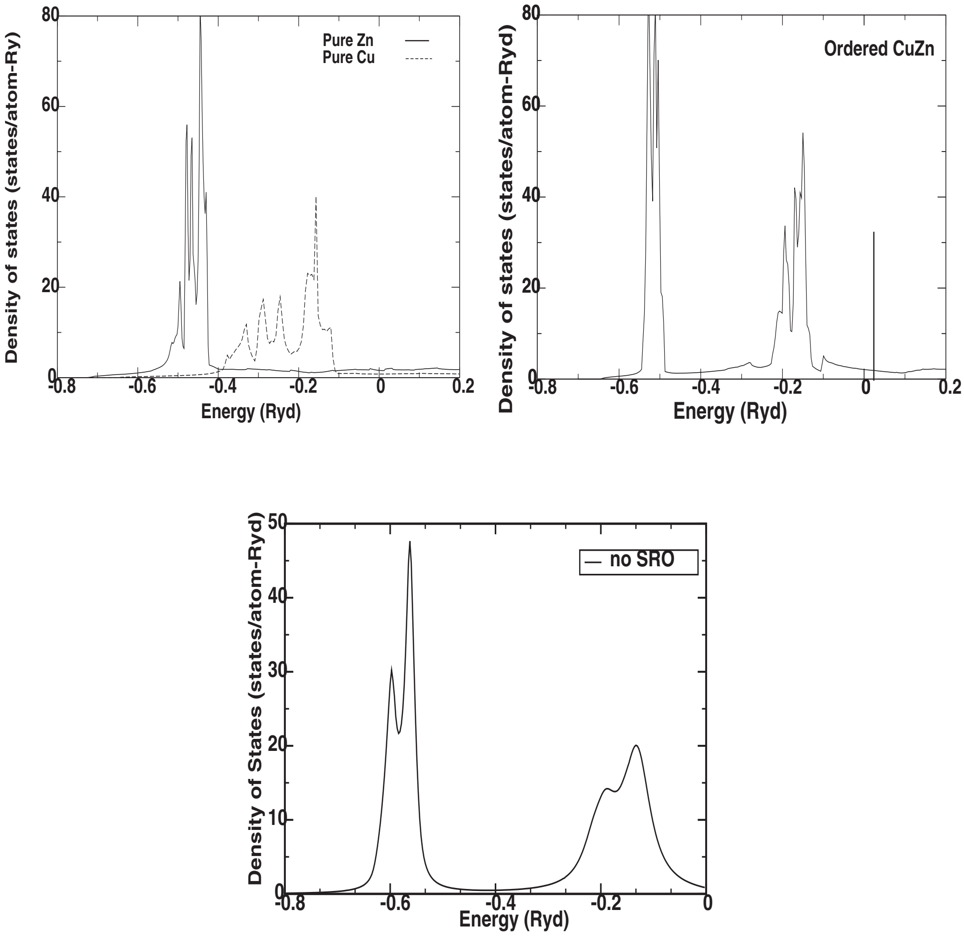

FIG. 2. (Top left) Density of states of pure Zn (solid lines) and Cu (dashed lines) in the same bcc lattice as the 50-50 CuZn alloy. (Top right) Density of states for ordered B2 50-50 CuZn alloy. (Bottom) Density of states for the disordered bcc 50-50 CuZn alloy.

The reason for this choice is that a considerable body of earlier work on CuZn exists using a plethora of different techniques. As a means of trying out the usefulness of our methodology, this system will provide enough other results for comparison.

The earliest first-principles density-functional-based study of the electronic properties of disordered CuZn was the single-site coherent potential approximation work of Bansil and Ehrenreich.[30] The authors studied the complex bands of α phase of CuZn using the KKR method. They commented on the significant effects of charge transfer on the electronic structure.

Later, using the much more sophisticated *locally self-consistent Green's function* (LSGF) approach based on the TB-LMTO technique, Abrikosov *et al.*[31] also studied CuZn alloys. The authors argued that earlier studies of the mixing enthalpies of CuZn using the standard CPA approaches[32,33] showed significant discrepancy with experiment. Part of the discrepancy was assumed to be from neglect of charge-transfer effects and part from the effects of SRO. Like our work, the main thrust of this technique, which was based on an earlier ideas of a locally self-consistent multiple scattering (LSMS) by Wang *et al.*,[34] was to go beyond the CPA and include the effects of the near environment of an atom in the solid. The LSMS gave an excellent theoretical estimate of the ordering energy in CuZn: 3.37 mRy/atom as compared to the experimental value of 3.5 mRy/atom.

Bruno *et al.*[35] proposed a modification of the CPA taking into account the local field and showed that charge-transfer effects can be taken into account accurately as compared to the O(N) methods just described. They applied their approach to the CuZn alloys.

We ourselves have applied the TB-LMTO-ASR technique to study CuZn.[36] The idea is very similar to this work. The effect of the configuration fluctuations of the environment of a site was captured through the recursion method. The effective medium was not "self-consistent" in the sense of a mean-field theory. In this paper we have suggested a way of obtaining this self-consistent effective medium.

For CuZn it would be interesting to address the effects of charge transfer and short-range ordering. In this application we shall address exactly these two points.

We have carried out the TB-LMTO-ASR calculations on CuZn with a lattice constant of 2.85 Å. The Cu and Zn potentials are self-consistently obtained via the LDA self-consistency loop. All reciprocal-space integrals are done by using the generalized tetrahedron integration for disordered systems introduced by us earlier.[37]

Figure 2 shows the densities of states for the pure Zn (solid lines) and Cu (dashed lines) in the same bcc lattice as the alloy and compares this with the ordered B2 and disordered bcc 50-50 CuZn alloy. We first note that in the ordered B2 alloy there is a considerable narrowing of the Zn well as the Cu *d*–like bands. The feature around −0.25 Ry is suppressed in the ordered alloy. In the disordered alloy on the other hand, although disorder scattering introduces lifetime effects which wash out the sharp structures in the ordered systems, the resemblance to the pure metals is evident.

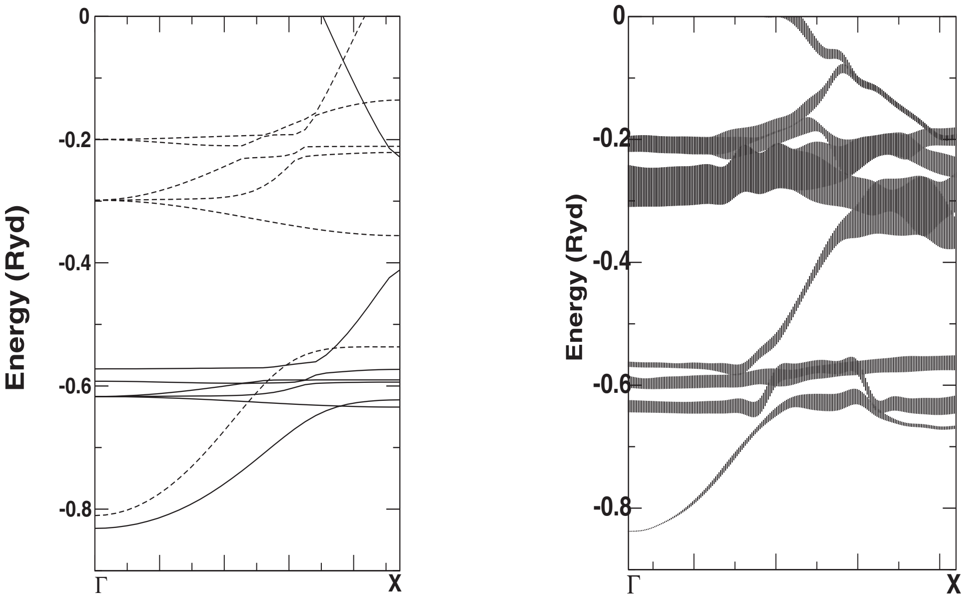

FIG. 3. (Left) Bands for pure Cu and Zn in bcc lattices with the same lattice parameter as the 50-50 CuZn alloy. The dashed lines are for Cu and the full lines are for Zn. (Right) Complex bands for the 50-50 CuZn alloy.

We have used the CCPA to obtain the complex bands from the spectral functions for the CuZn alloy. This is shown in Fig. 3. The results are very closely similar to the ASR results. This is expected as the two approaches have much in common.

The two panels of Fig. 3 compare the band structures of pure Cu and pure Zn metals in the same bcc lattice as the 50-50 alloy. We note that the *s*-like bands of Cu and Zn stretch from −0.8 Ry, while the *d*-like states of Zn and Cu, whose degeneracies are lifted by the cubic symmetry of the bcc lattice, are more localized and reside in the neighborhood of −0.6 Ry and between −0.3 and −0.2 Ry, respectively. The complex bands of the solid clearly reflect the same band structure. However, the bands are slightly shifted and broadened because of the disorder scattering of Bloch states in the disordered alloy. The scattering lifetimes are maximum for the Cu *d*–like bands, less for the Zn *d*–like bands, and minimum for the lower *s*-like bands. This is expected since the delocalized *s*-like states straddle large volumes of the lattice space and are therefore less sensitive to the local configuration fluctuations of the substitutional alloy.

We comment here that the complex band structure very closely resembles that obtained through the TB-LMTO-ASR by us earlier.[36] This is expected because the two approaches are very similar, differing only in the way the effect of the far environment is taken into account.

Let us now turn to the study of the effect of SRO, leading, on one hand, to ordering ($\alpha < 0$) and, on the other hand, to segregation ($\alpha > 0$). We shall look at Figs. 2 and 3. The complex band structure (shown in Fig. 3) indicates that the system is a *split-band* alloy. The positions of the *d* bands of Cu and Zn are well separated in energy. This implies that the "electrons travel more easily between Cu or between Zn sites than between unlike ones."[8] So when the alloy orders and

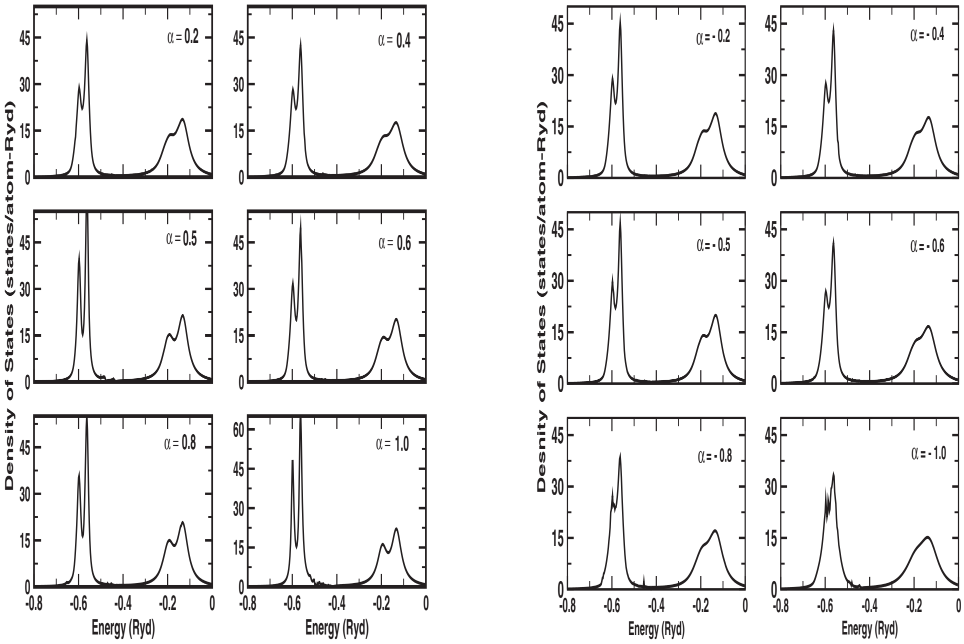

FIG. 4. Densities of states with different degrees of SRO leading to clustering (left two panels) and ordering (right two panels).

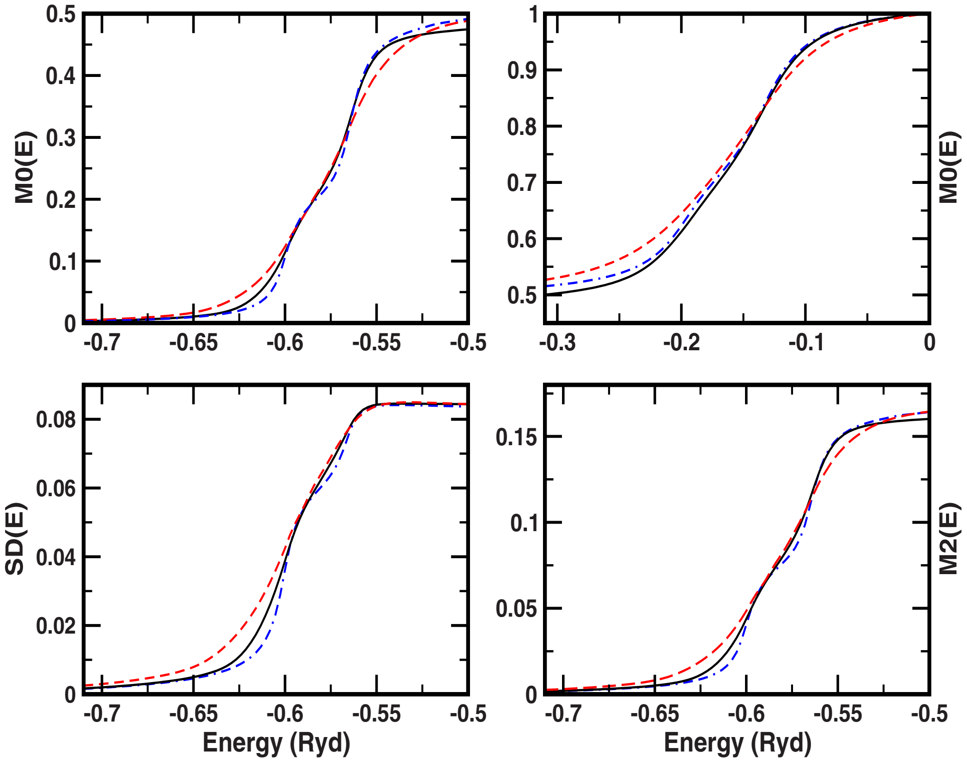

FIG. 5. (Color online) (Top) The integrated density of states for the two bands of CuZn. (Bottom) The variation and second moment of the density of states of the lower-energy band. Black full curves refer to the case without SRO, red dashed curves refer to $\alpha=1$ (clustering), and blue dashed-dotted curves to $\alpha=-1$ (ordering).

unlike sites sit next to each other, the overlap integral between the like sites decrease. This leads to a narrowing of the bands associated with Cu and Zn. A comparison between the top left and top right panels of Fig. 2 clearly shows that the bands in the latter are narrower as compared to the former. This is the main effect of the onset of order. On the other hand, when the alloy is completely disordered, the bands get broadened by disorder scattering and the sharp structure in the density of states are smoothed.

The left two panels of Fig. 4 show the density of states with increasing positive α. Positive α indicates a clustering tendency. Comparing with Fig. 2 we note that as clustering tendency increases the density of states begins to show the structures seen in the pure metals in both the split bands. For large positive α there is still residual long-range disorder. This causes smoothing of the bands with respect to the pure materials. For these large, positive α's, we notice the development of the structure around -0.25 Ry.

The right two panels of Fig. 4 show the density of states with increasing negative α, which indicates increasing ordering tendency. On the bcc lattice at 50-50 composition we expect this ordering to favor a B2 structure. With increasing ordering tendency, both the split bands narrow and lose structure. The feature around -0.25 Ry disappears. This band narrowing and suppression of the feature around -0.25 Ry is clearly seen in the ordered B2 alloy shown in Fig. 2.

A more quantitative analysis of the effect of SRO on the shape of the density of states uses the moment functions

$$M_n(E) = \int_{-\infty}^{E} dE'(E')^n n(E').$$

In particular one may use the integrated density of states $M_0(E)$ and the second moment and "variation" in spectral distribution, $M_2(E)$ and $\mathrm{SD}(E)=M_2(E)-M_1^2(E)$. These are shown in Fig. 5 for the cases of no SRO, perfect clustering $\alpha=1$, and ordering $\alpha=-1$. $M_0(E)$ shows a left shift of spectral weight toward -0.6 Ry in the lower band as clustering tendency increases. In the upper band there is a spectral shift around -2.0 to -3.0 Ry range, which gives rise to the characteristic shoulder around those energies. For ordering $M_0(E)$ indicates a right shift of spectral weight toward -0.55 Ry. SD(E) indicates a distribution of spectral weight away from the mean on clustering and a bunching of spectral weight toward the mean on ordering. The latter indicates a narrowing of the density of states. Use of moment functions quantifies the comparison of the changes in the shapes of the density of states with clustering or ordering.

ACKNOWLEDGMENTS

M.R. would like to thank TWAS, Trieste, Italy for financial assistance.

*abhijit@bose.res.in

[1] A complex function $f(z)$ is called *Herglotz* if (a) its singularities lie on the real z axis, (b) $\text{sgn}[\text{Im} f(z)]=-\text{sgn}(\text{Im} z)$, and (c) $f(z) \sim 1/z$ as $z \rightarrow \pm\infty+i0$.

[2] S. S. A. Razee and R. Prasad, Phys. Rev. B **45**, 3265 (1992).

[3] S. S. A. Razee and R. Prasad, Phys. Rev. B **48**, 1349 (1993).

[4] S. Ghosh, P. L. Leath, and M. H. Cohen, Phys. Rev. B **66**, 214206 (2002).

[5] A. Chakrabarti and A. Mookerjee, Eur. Phys. J. B **44**, 21 (2005).

[6] A. Zunger, S.-H. Wei, L. G. Ferreira, and J. E. Bernard, Phys. Rev. Lett. **65**, 353 (1990).

[7] M. Jarrell and H. R. Krishnamurthy, Phys. Rev. B **63**, 125102 (2001).

[8] D. A. Rowlands, J. B. Staunton, B. L. Gyorffy, E. Bruno, and B. Ginatempo, Phys. Rev. B **72**, 045101 (2005).

[9] The partitioning theorem states that if we partition a Hilbert space $\mathcal{H}=\mathcal{H}_1 \cup \mathcal{H}_2$ and $\mathcal{H}_1 \cap \mathcal{H}_2=\emptyset$, then if H is an operator in $\mathcal{H}$, then $H^{-1}=(H_1+H'^T H_2^{-P_2} H')^{-P_1}$, where $-P_j$ denotes the inverse in the subspace $\mathcal{H}_j$, while $H_j=P_j H P_j$ and $H'=P_j H P_{j'}$. P_j is the projection operator onto the subspace $\mathcal{H}_j$.

[10] R. Haydock, Philos. Mag. B **43**, 203 (1981); R. Haydock and R. L. Te, Phys. Rev. B **49**, 10845 (1994).

[11] R. Haydock, Ph.D. thesis, University of Cambridge, 1972.

[12] N. Beer and D. G. Pettifor, in *The Electronic Structure of Complex Systems*, edited by P. Phariseau and W. M. Temmerman (Plenum, New York, 1984), p. 769.

[13] A. Datta, P. K. Thakur, and A. Mookerjee, Phys. Rev. B **48**, 8567 (1993).

[14] A. Gonis and J. W. Garland, Phys. Rev. B **16**, 2424 (1977).

[15] J. S. Faulkner, in *Progress in Materials Science*, edited by J. W. Christian, P. Hassen, and T. Massalski (Pergamon, New York, 1982), Vol. 27, p. 1.

[16] W. Kohn and L. J. Sham, Phys. Rev. **140**, A1133 (1965).

[17] O. K. Andersen and O. Jepsen, Phys. Rev. Lett. **53**, 2571 (1984).

[18] A. Mookerjee, in *Electronic Structure of Clusters, Surfaces and Disordered Systems*, edited by A. Mookerjee and D. D. Sarma (Taylor & Francis, London, 2003).

[19] A. Mookerjee, J. Phys. C **6**, 1340 (1973).

[20] The following notation has been adopted: unmarked operators X act on the space $\mathcal{H}$ spanned by the LMTO basis. Hatted operators $\hat{X}$ act on the configuration space Φ and tilded operators $\widetilde{X}$ act on the augmented space $\mathcal{H} \otimes \Phi$.

[21] See EPAPS Document No. E-PRBMDO-79-092901 for details of the derivation of the CCPA equations. For more information on EPAPS, see http://www.aip.org/pubservs/epaps.html.

[22] S. S. A. Razee, A. Mookerjee, and R. Prasad, J. Phys.: Condens. Matter **3**, 3301 (1991).

[23] T. Saha, I. Dasgupta, and A. Mookerjee, Phys. Rev. B **50**, 13267 (1994).

[24] T. Saha, I. Dasgupta, and A. Mookerjee, J. Phys.: Condens. Matter **8**, 1979 (1996).

[25] R. Haydock, V. Heine, and M. J. Kelly, J. Phys. C **5**, 2845 (1972).

[26] R. Haydock, *Solid State Theory* (Academic, New York, 1980), Vol. 35.

[27] R. Mills and P. Ratanavararaksa, Phys. Rev. B **18**, 5291 (1978).

[28] R. Mills, L. J. Gray, and T. Kaplan, Phys. Rev. B **27**, 3252 (1983).

[29] A. Mookerjee and R. Prasad, Phys. Rev. B **48**, 17724 (1993).

[30] A. Bansil, H. Ehrenreich, L. Schwartz, and R. E. Watson, Phys. Rev. B **9**, 445 (1974).

[31] I. A. Abrikosov, A. E. Kissavos, F. Liot, B. Alling, S. I. Simak, O. Peil, and A. V. Ruban, Phys. Rev. B **76**, 014434 (2007).

[32] I. A. Abrikosov, Yu. H. Velikov, P. A. Korzhavyi, A. V. Ruban, and L. E. Shilkrot, Solid State Commun. **83**, 867 (1992).

[33] P. A. Korzhavyi, A. V. Ruban, I. A. Abrikosov, and H. L. Skriver, Phys. Rev. B **51**, 5773 (1995).

[34] Y. Wang, G. M. Stocks, W. A. Shelton, D. M. C. Nicholson, Z. Szotek, and W. M. Temmerman, Phys. Rev. Lett. **75**, 2867 (1995).

[35] E. Bruno, L. Zingales, and A. Milici, Phys. Rev. B **66**, 245107 (2002).

[36] K. Tarafder, A. Chakrabarti, K. K. Saha, and A. Mookerjee, Phys. Rev. B **74**, 144204 (2006).

[37] K. K. Saha, A. Mookerjee, and O. Jepsen, Phys. Rev. B **71**, 094207 (2005).